Dispersion Studies in THz Plasmonic Devices with Cavities

Mustafa Karabiyik[*,a], Raju Sinha[a], Chowdhury Al-Amin[a], Gregory C. Dyer[b], Nezih Pala[a], Michael S. Shur[c]
[a] Electrical and Computer Engineering, Florida International University, 10555 W Flagler St., Miami, FL, USA, 33174, US
[b] Sandia National Laboratories, P.O. Box 5800, Albuquerque, New Mexico 87185, US
[c] Department of Electrical, Computer, and Systems Engineering and Physics, Applied Physics and Astronomy, Rensselaer Polytechnic Institute, Troy, New York 12180, US

ABSTRACT

Analytical and numerical studies of the dispersion properties of grating gated THz plasmonic structures show that the plasmonic crystal dispersion relation can be represented in terms of effective index of the dielectric medium around the 2DEG for the plasmons. Forbidden energy band gaps are observed at Brillion zone boundaries of the plasmonic crystal. FDTD calculations predict the existence of the plasmonic modes with symmetrical, anti-symmetrical and asymmetrical charge distributions. Breaking the translational symmetry of the crystal lattice by changing the electron concentration of the two dimensional electron gas (2DEG) under a single gate line in every 9-th gate induces a cavity state. The induced cavity state supports a weekly-coupled cavity mode.

Keywords: Terahertz, plasmon, 2DEG, dispersion, plasmonic crystal, cavity, AlGaN/GaN.

1. INTRODUCTION

Plasma oscillations in various types of field effect transistors[1,2] (FETs) are used for THz detection,[3,4,5,6,7] mixing, [8,9,10] and generation.[11,12] Plasmonic THz detectors have the advantage of continuous tunability over the conventional detectors such as bolometers and pyroelectric detectors.[13]

The 2DEG based high electron mobility field effect transistors (HEMTs) are capable of supporting two types of THz plasmons: gated and ungated plasmons.[15] The gated region of a FET supports gated plasmons with electromagnetic fields confined in between the 2DEG and the gate, while ungated plasmons with a different dispersion law are observed in the ungated region of a FET. In the case of periodically spaced gates, the grating gate supplies the necessary momentum to excite the plasmons compensating the momentum mismatch between the THz waves in free space and plasmons.

In order to understand the physical properties of THz plasmons in FETs, the dispersion relations has been developed for gated 2DEG structures and ungated 2DEG structures as well as a combination of these two structures into a lattice with one-dimensional (1D) translational symmetry, known as a 1D plasmonic crystal. The gated or ungated plasmon dispersions for isolated gated and ungated regions neglect the coupling between these regions.[14] Recent studies have shown that the dispersion can be solved for plasmonic crystals, but the presented solutions are either an analogy to electrical circuits or to electronic wave solutions.[15-16] Here we present the description of the plasmonic crystal dispersion relation that is framed in the context of the optical properties of the THz plasmons.

2. THEORY

A 1D plasmonic crystal (see Fig. 1) is a 1D periodic structure that consists of two different regions with different effective indices of n_1 and n_2 resulting in two different plasmon wave velocities. This produces plasmonic band gaps due to scattering of plasma waves at the interfaces between the two regions, provided that the Bragg condition is satisfied

* mustafa.karabiyik@fiu.edu

Terahertz Physics, Devices, and Systems VIII: Advanced Applications in Industry and Defense, edited by Mehdi F. Anwar, Thomas W. Crowe, Tariq Manzur, Proc. of SPIE Vol. 9102, 91020K

$$k_P = G/2 \tag{1}$$

where k_P is the momentum of the plasmons and $G=2\pi/L$ is the reciprocal lattice vector, with L is the period of the grating.[17] The non-identical effective indices result from differences in plasmon screening in the gated and ungated regions of the THz plasmonic structure, and depend on the excitation frequency, structure geometry, and the refractive index of the intrinsic semiconductor material in which the 2DEG is embedded.

Kachorovskii and Shur have shown that the plasmonic crystal dispersion relation can be solved for the case of two different gated regions with non-identical wave velocities.[16-17] The effective index of the plasmons describes the velocity of the plasmons; the analogy was made by considering that the plasmons have two different velocities in ungated and gated regions. This case can be converted into an optical formalism by representing the plasmon wave velocity at ungated region 'a' as $S_a=c/n_a$ and the plasmon wave velocity at gated region 'b' as $S_b=c/n_b$ where c is speed of light and n_a and n_b are the effective indices at different regions. In our case, n_a and n_b are the effective indices at ungated and gated regions. The modified equation then is stated in an optical description of the plasmonic system describing surface polariton-plasmonic (SPP) modes:

$$k(f) = \frac{1}{L_a+L_b} arccos\left[cos\frac{2\pi f L_a n_a}{c} cos\frac{2\pi f L_b n_b}{c} - \frac{n_a^2+n_b^2}{2n_a n_b} sin\frac{2\pi f L_a n_a}{c} sin\frac{2\pi f L_b n_b}{c}\right] \tag{2}$$

where f is the frequency, L_a and L_b are the length of gated and ungated region.

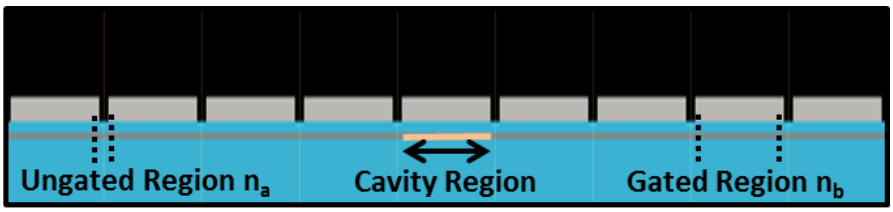

Fig. 1: Schematic representation of a grating gate plasmonic device with cavity with semi-infinite crystal on either side. The ungated region has an effective index of n_a and gated region has an effective index of n_b. The cavity region is represented with a different color over the 2DEG. The cavity is repeated in every 9 gratings.

Cavity states can also emerge in plasmonic crystal structures where there is breaking of the translational symmetry. In the case of grating gated devices, a cavity element may be introduced into the periodic structure by applying a non-identical gate voltage to one grating element that changes the electron concentration underneath. Such cavities can localize plasmons due to the wave velocity change upon reflection. In Fig. 1, we show a cavity structure that is achieved by applying a voltage in every 9 elements periodically to the grating gate elements. [18,19,20,21] For an isolated cavity, the cavity state is dispersionless. For cavities that are in close proximity of each other, SPP modes can couple to each other. Coupling of such cavities shows dispersion. When cavities are in close proximity and they are coupled, the dispersion obtained from the analog of the tight binding approximation is;

$$\omega(k) = \alpha[1 + \beta\cos(kD)] \tag{3}$$

where D, α, β, k are superperiodicity (cavity to cavity distance) of the cavities, resonance frequency of individual cavity, coupling factor and momentum of SPP respectively. [22] The resonance condition is given by

$$\delta=(2n+1)(\lambda_P/4) \tag{4}$$

where δ is the phase shift added to the plasmons while traveling over the cavity element, n is the order of the cavity resonance and a positive integer starting from zero, λ_p is the wavelength of the plasmon.

3. SIMULATION MODEL

A commercial FDTD simulation tool, Lumerical, is used to investigate the electromagnetic field profile of the plasmons and the dispersion of 2D plasmons at THz frequencies.[23] The modes are excited using a dipole source with

polarization perpendicular to the gratings under different energy and momentum configurations. The plasmons are excited when the momentum and energy of the incident wave is matched with the plasmons. A monitor is placed around the channel to calculate the excitation spectrum of the plasmons. An electric field profile monitor is placed to record the electric field profile of the plasmons. The 2DEG is defined as a plasma layer with specific plasma frequency and collision frequency extracted from the experimental results with higher mobility.[24] The simulation is automatically stopped when the total electric field converges down to an amplitude that is orders of magnitude smaller than the incident field.

4. DISPERSION

4.1 Uniform Grating Gate

The dispersion of plasmons in grating gate devices is studied. The device model is considered as a GaN/AlGaN HEMT device. The mobility used is the high electron mobility at low cryogenic temperatures, typically below liquid nitrogen temperatures of 77 K, in order to excite high quality factor plasmons and distinguish plasmonic modes properly. If the mobility is too low, the modes are broadened in energy and cannot be individually resolved.

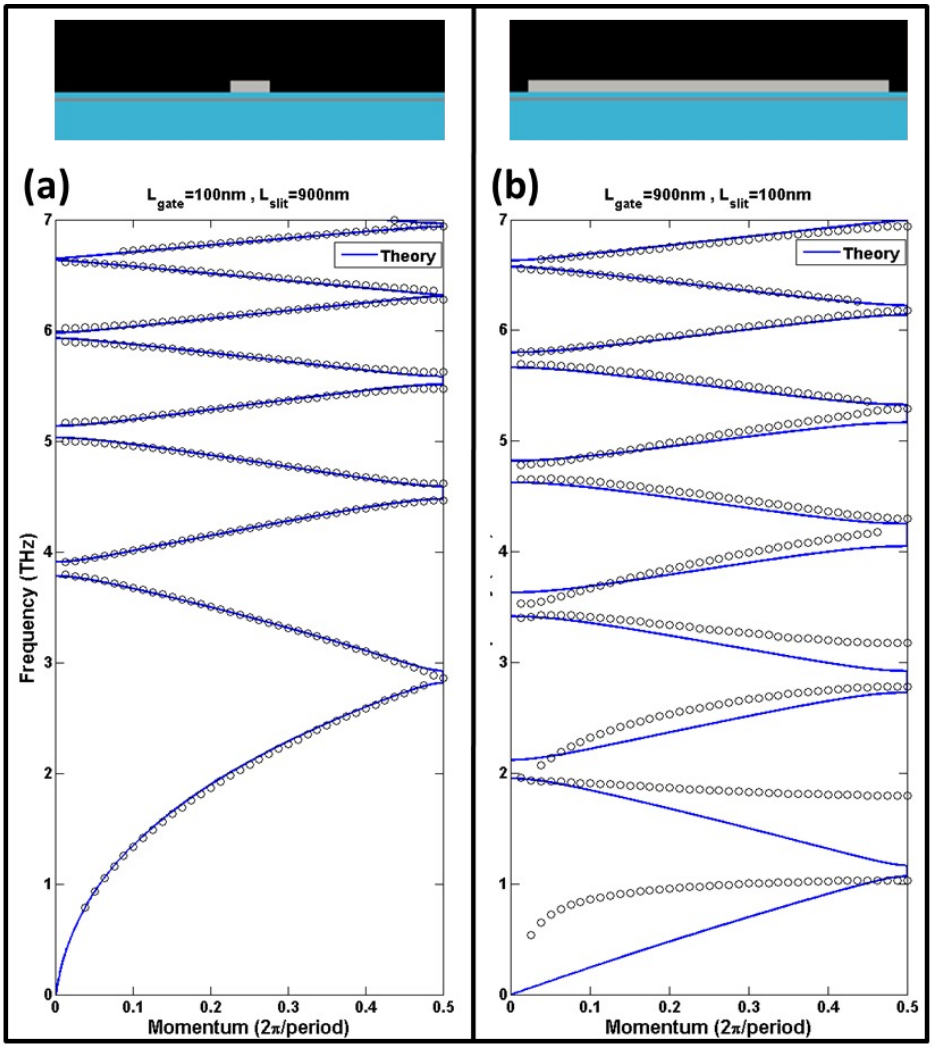

Fig. 2: Dispersion curves of grating gate 2D plasmonic devices. The blue solid line is the analytical dispersion and circled points are the calculated points by FDTD method. (a) Grating gate device with 100 nm gate length and 900 nm slit length. (b) Grating gate device with 900 nm gate length and 100 nm slit length.

Two grating geometries where studied. One has a 100 nm gate length with a 900 nm ungated slit, and the other has a 900 nm gate length with a 100 nm ungated slit. The gate-channel separation is 30 nm in both geometries. Both geometries are represented in Fig. 2. Fig. 2 compares the analytical and numerical dispersion.. While Fig. 2 (a) is in good agreement with analytical calculations, Fig. 2 (b) has a mismatch at lower frequencies. The effective indices are calculated via FDTD mode calculation method by taking the cross section of gated and ungated regions. The gated modes at lower frequencies are highly screened by the gate while lower frequency modes tend to be closer to 2DEG with less screening. This causes a dramatic index modulation of the low frequency modes, which is not considered in the analytical calculation. A better 2-dimensional effective index calculation is necessary for a better fit for Fig. 2 (b). The dispersion curves of the grating gated devices show that a band gap is opened up in several energy bands. There are no propagating plasmonic modes with purely real crystal wave vectors within the band gap.

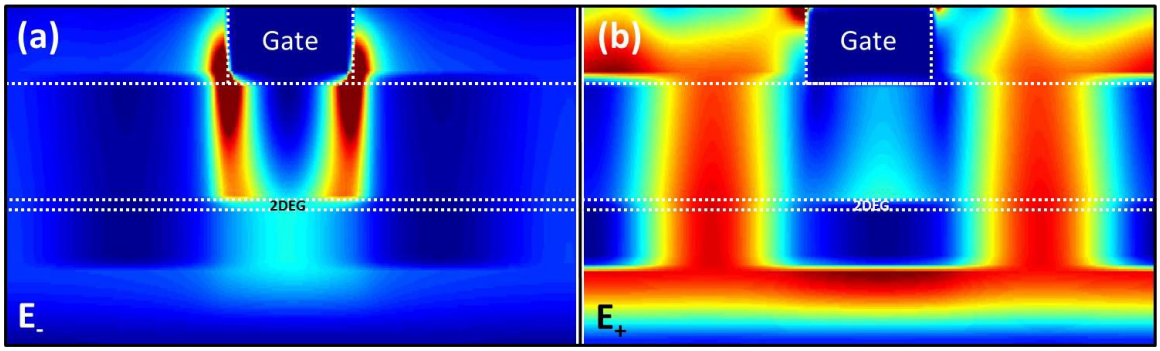

Fig. 3: Electric field distributions ($|E|^2$) at the band edges for the grating gate device with 100 nm gate length and 900 nm slit length. The momentum is zero for both cases. E_- has a frequency of 3.8 THz while the E_+ has a frequency of 3.9 THz. Red indicates the high electric fields and blue indicates the low electric field. Both of the modes are anti-symmetric modes.

Plasmon Bragg scattering in the periodic structure results in both forward and backward traveling waves that interfere constructively to form a standing wave profile. Plasmons with momentum of G/2 interfere constructively in the structure forming two standing wave profiles with different energies at the band edges. The minima of the high energy standing wave form in the lower effective index region, E_+ and the maxima of the low energy standing wave occur in the high index region E_-. Plasmons with energies in between the forbidden energy bands interfere destructively and plasmon propagation is not allowed along the structure. [25] Hence, a band gap is formed, known as the plasmonic band gap. The ungated cavity and gated cavity form one larger compound cavity, and they cannot be considered as two isolated cavities adjacent to each other. They are strongly coupled as seen from the plasmonic field profile in Fig. 3.

The energy of the E_+ and E_- modes is related to the distortion in the electric field lines. This distortion depends on the gated and ungated region effective index contrast. The band gap span also depends on this effective index contrast. Therefore, as the grating gate length increases, we expect for the band gap to be widened as seen in Fig. 3.[26]

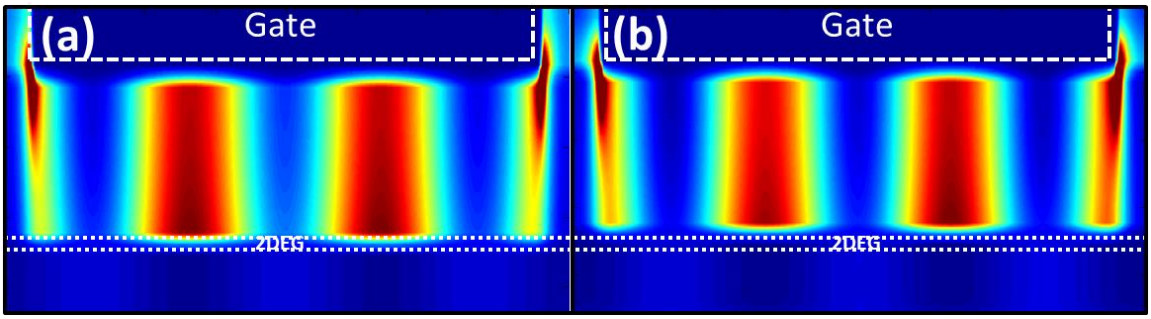

Fig. 4: Electric field distributions ($|E|^2$) at the 3rd branch of the band for the grating gate device with 900 nm gate length and 100 nm slit length. The momentum is 0.25 2π/period, frequency is 2.6 for (a) and the momentum is 0.375 2π/period, frequency 2.7 THz for (b). Red indicates the high electric fields and blue indicates the low electric field.

Fig. 4 shows the electric field distributions of 2 different frequency-momentum configurations. Fig. 4 (a) is an example for symmetric mode and Fig. 4 (b) is an example for asymmetric mode. While the field distribution in quarter momentum is totally symmetric, the field distribution at momentum 3/8 is asymmetric. There is an intensity difference between the central peaks.

4.2 Grating Gate with Cavity

To study the formation of cavities in plasmonic crystals with broken translational symmetry, we used a model where an electron concentration of 90% of the surrounding 2DEG occurs below every 9th gate. Experimentally, a grating structure with different electron concentration can be achieved by applying a voltage to the corresponding gates in a super periodic manner. It might also occur due to the variations of the threshold voltage from a gated region to a gated region. Fig. 5 shows the dispersion relation for a grating gate device with a 900 nm gate length and a 100 nm slit length. The horizontal axis is the plasmon momentum and the vertical axis is the plasmon frequency. The dispersion is only shown in and near the first band gap because a cavity state is expected to be observed within this band gap. A dispersionless mode is observed at 1.7 THz in contrast to Fig. 2. (b) where it as absent. The additional plasmonic mode is the first excited cavity mode within the band gap. The corresponding electric field distributions at a momentum of 0.5 of the grating are shown for two branches and the cavity mode in Fig. 5.

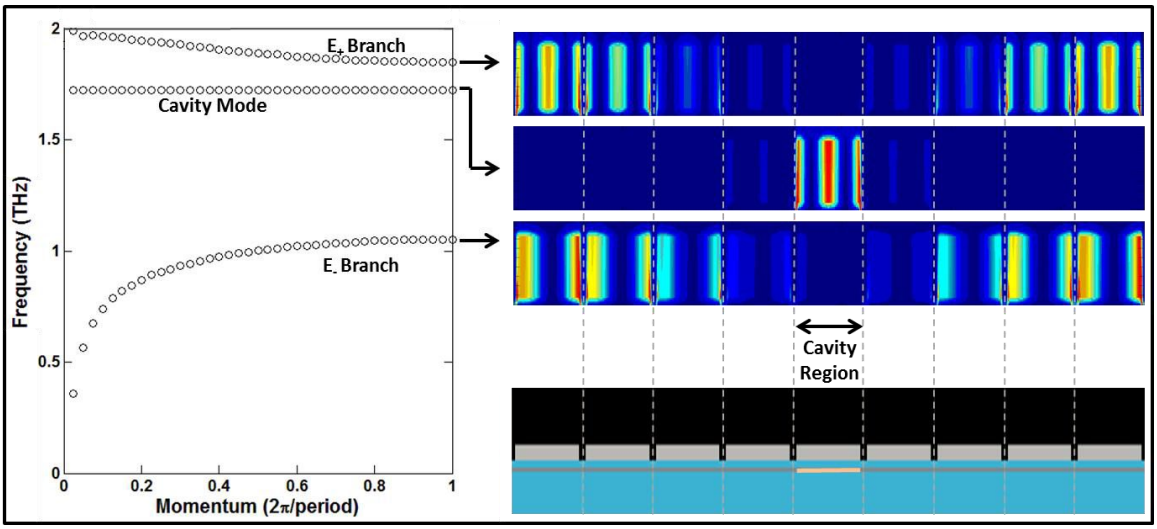

Fig. 5: Dispersion curve of grating gate 2D plasmonic devices with cavities. Grating gate device geometry has 900 nm gate length and 100 nm slit length. Electric field distributions ($|E|^2$) of the corresponding branches are shown. Red indicates the high electric fields and blue indicates the low electric field. Cavity mode is localized on the cavity region while resonant modes are localized on off-cavity regions.

Optical cavities that localize light in the forbidden band gap can be obtained by breaking the symmetry of a photonic crystal.[27-28] High transmission bands at frequencies within the band gap of the photonic crystal can be achieved.[29] New electromagnetic modes in the cavities are created due to the constructive interference of the photons for wavelengths within the cavity region.

Fig. 5 shows the electric field distributions of the plasmonic modes for each corresponding plasmonic mode branch at the band edge. The blue regions on the graph show the plasmon electric field distribution minima while the red regions represent the maxima. A plasmonic cavity state is created around 1.7 THz. The gap can be identified in between 1 THz and 1.8 THz. From Fig. 5, it is clear that the slope of the cavity state defines a standing wave since the derivative of the dispersion is zero corresponding to the zero group velocity, which is the indication of a standing wave profile. The group velocity of the cavity state indicates that, for our configuration, the cavities are weekly coupled.

To see how plasmonic cavity mode localizes at the cavity structures, the electric field intensity profiles of the cavity mode have been simulated. The electric field intensity distribution is shown in Fig. 5 for the first cavity mode supported by the structure. The field distributions show that the electric field peaks are located within the cavity regions, which are excited at the resonant frequencies supported by the cavity structure. The resonant modes are

widely distributed over the uniform grating side while creating an interference pattern that is the highest at the center of the uniform grating region. By controlling the electron concentration of the cavity structure, the resonance condition can be tuned.[29]

5. CONCLUSION

The 2D plasmonic crystal dispersion relation is represented in terms of the effective index of plasmons in two elements that form the primitive crystal unit cell. The dispersion of grating gated plasmonic structures shows band gaps at the Brillion zone boundaries. A cavity is induced by changing the electron concentration of a single gate stripe in every 9 gates embedded in a plasmonic crystal and the plasmonic cavity mode is observed in FDTD simulations. These results suggest that the cavity states might be used for creating narrow bands of resonant frequencies for resonant THz detectors using plasmonic crystals.

Acknowledgements

This work is supported by NSF CAREER program with the Award Number: 1149059 and Army Research Laboratory (ARL) Multiscale Multidisciplinary Modeling of Electronic Materials (MSME) Collaborative Research Alliance (CRA) (Grant No. W911NF-12-2-0023, Program Manager: Dr. Meredith L. Reed). The authors would like to acknowledge the Instructional & Research Computing Center (IRCC) at Florida International University for providing HPC computing resources that have contributed to the research results reported within this paper, web: http://ircc.fiu.edu.

The work at Sandia National Laboratories was supported by the DOE Office of Basic Energy Sciences. This work was performed, in part, at the Center for Integrated Nanotechnologies, a U.S. Department of Energy, Office of Basic Energy Sciences user facility. Sandia National Laboratories is a multi-program laboratory managed and operated by Sandia Corporation, a wholly owned subsidiary of Lockheed Martin Corporation, for the U.S. Department of Energy's National Nuclear Security Administration under contract DE-AC04-94AL85000.

Raju Sinha gratefully acknowledges the financial support provided by the Presidential Fellowship from Florida International University Graduate School.

REFERENCES

[1] Dyakonov M. and Shur M.S., "Plasma wave electronics: novel terahertz devices using two dimensional electron fluid" IEEE Trans. Electron Devices 43, 380 (1996).

[2] Shur M.S. and Lu J.Q., "Terahertz Sources and Detectors Using Two-Dimensional Electronic Fluid in High Electron-Mobility Transistors" EEE Trans. Microwave Theory and Techniques 48, 750 (2000).

[3] Knap W., Deng Y., Rumyantsev S., Lu J.-Q., Shur M. S., Saylor C. A., and Brunei L. C. "Resonant detection of subterahertz radiation by plasma waves in a submicron field-effect transistor" Appl. Phys. Lett. 80, 3433 (2002).

[4] Peralta X. G., Allen S. J., Wanke M. C., Harff N. B., Simmons J. A., Lilly M. P., Reno J. A., Burke P. J., and. Eisenstein J. P "Terahertz photoconductivity and plasmon modes in double-quantum-well field-effect transistors" Appl. Phys. Lett. 81, 1627 (2002).

[5] Satou A., Khmyrova I., Ryzhii V., and Shur M. S., "Plasma and transit-time mechanisms of the terahertz radiation detection in high-electron-mobility transistors" Semicond. Sci. Technol 18, 460 (2004).

[6]Teppe F., Knap W., Veksler D., Dmitriev A. P., Kachorovskii V. Y., Rumyantsev S., and Shur M. S. "Room-temperature plasma waves resonant detection of sub-terahertz radiation by nanometer field-effect transistor" Appl. Phys. Lett. 87, 052107 (2005).

[7] Shaner E. A., Lee M., Wanke M. C., Grine A. D., Reno J. L., and Allen S. J., "Single-quantum-well grating-gated terahertz plasmon detectors" Appl. Phys. Lett. 87, 193507 (2005).

[8] Veksler D., Teppe F., Dmitriev A. P., Kachorovskii V. Yu., Knap W., and Shur M. S., "Detection of terahertz radiation in gated two-dimensional structures governed by dc current" Phys. Rev. B 73, 125328 (2006).

[9] Ryzhii V., Khmyrova I., Satou A., Vaccaro P. O., Aida T., and Shur M., "Plasma mechanism of terahertz photomixing in high-electron mobility transistor under interband photoexcitation" J. Appl. Phys. 92, 5756 (2002).

[10] Satou A., Ryzhii V., Khmyrova I., and Shur M.S., "Characteristics of a terahertz photomixer based on a high-electron mobility transistor structure with optical input through the ungated regions" J. Appl. Phys. 95, 2084 (2005).

[11] Lee M., Wanke M. C., and Reno J. L., "Millimeter wave mixing using plasmon and bolometric response in a double-quantum-well field-effect transistor" Appl. Phys. Lett. 86, 033501 (2005).

[12] Knap W., Lusakowski J., Parenty T., Bollaert S., Cappy A., "Terahertz emission by plasma waves in 60 nm gate high electron mobility transistors" Appl. Phys. Lett. 84, 2331 (2004).

[13] Dyakonova N., Teppe F., Łusakowski J., Knap W., Levinshtein M., "Magnetic field effect on the terahertz emission from nanometer InGaAs/AlInAs high electron mobility transistors" J. Appl. Phys. **97**, 114313 (2005).

[14]Popov V. V., Polischuk O. V., Shur M. S., "Resonant excitation of plasma oscillations in a partially gated two-dimensional electron layer", Journal of Applied Physics, 98, 033510 (2005)

[15] Aizin, G. R., and Dyer, G. C., "Transmission line theory of collective plasma excitations in periodic two-dimensional electron systems: Finite plasmonic crystals and Tamm states," Phys. Rev. B, 86(23), 235316 (2012).

[16] Kachorovskii, V. Yu; Shur, M.S., "Current-induced terahertz oscillations in plasmonic crystal," *Applied Physics Letters* , vol.100, no.23, pp.232108,232108-4, Jun 2012

[17] C Kittel., [Introduction to Solid State Physics, 8th Edition], John Wiley & Sons Inc., New York, 164-180 (1986).

[18] Dyer, G. C., Aizin, G. R., Preu, S., Vinh, N. Q., Allen, S. J., Reno, J. L., and Shaner, E. A., "Inducing an Incipient Terahertz Finite Plasmonic Crystal in Coupled Two Dimensional Plasmonic Cavities," Phys. Rev. Lett., 109(12), 126803 (2012).

[19]Dyer G. C., Vinh N. Q., Allen S. J., Aizin G. R., Mikalopas J., Reno J. L., and Shaner E. A., "A terahertz plasmon cavity detector," Appl. Phys. Lett. 97, 193507 (2010).

[20]Dyer G. C., Preu S., Aizin G. R., Mikalopas J., Grine A. D., Reno J. L., Hensley J. M., Vinh N. Q., Gossard A. C., Sherwin M. S., Allen S. J., and Shaner E. A., "Enhanced performance of resonant sub-terahertz detection in a plasmonic cavity," Appl. Phys. Lett. 100, 083506 (2012).

[21]Davoyan A. R., Popov V. V., and Nikitov S. A. "Tailoring Terahertz Near-Field Enhancement via Two-Dimensional Plasmons" Phys. Rev. Lett. 108, 127401 (2012).

[22]Yariv A., Xu Y., Lee R. K., and Scherer A. "Coupled resonator optical waveguide: A proposal and analysis" June 1, Vol.24, No.11 Optics Letters (1999).

[23] Lumerical Solutions Inc., Vancouver, Canada.

[24] Muravjov A. V., Veksler D. B., Popov V. V., Polischuk O. V., Pala N., Hu X., Gaska R., Saxena H., Peale R. E., and Shur M. S., "Temperature dependence of plasmonic terahertz absorption in grating-gate gallium-nitride transistor structures" Applied Physics Letters, 96, 042105 (2010).

[25]Barnes W. L., Preist T. W., Kitson S. C., and Sambles J. R. "Physical origin of photonic energy gaps in the propagation of surface SPPs on gratings" Physical Review B, Volume 54, Number 9, 6227-6244 (1996).

[26]Fischer B., Fischer T. M., and Knoll W. "Dispersion of surface-plasmons in rectangular, sinusoidal, and incoherent silver gratings" J. Appl. Phys. 75, 1577 (1994).

[27]Yablonovitch E., Gmitter T.J., Meade R.D., Rappe A.M., Brommer K.D. and Joannopoulos J.D. "Donor and acceptor modes in photonic band structure" Phys. Rev. Lett. 67, 3380 (1991).

[28]Dyer G. C., Aizin G. R., Allen S. J., Grine A. D., Bethke D., Reno J. L., and Shaner E. A., "Induced transparency by coupling of Tamm and defect states in tunable terahertz plasmonic crystals," Nature Photon. **7**, 925-930 (2013).

[29]Bayindir M., Temelkuran B., and Ozbay E. "Tight-Binding Description of the Coupled Defect Modes in Three-Dimensional Photonic Crystals" Phys. Rev. Lett. 84, 2140–2143 (2000).